CONF-821074--1

CONF-821074--1

DE83 001962

RECENT DEVELOPMENTS IN POSITION-SENSITIVE NEUTRON COUNTING*

K. H. Valentine, M. K. Kopp, G. C. Guerrant and J. A. Harter

Oak Ridge National Laboratory,
Oak Ridge, Tennessee 37830, USA

1. INTRODUCTION

Continuing research on advanced methods of thermal neutron detection and position sensing with gas-filled counters was aimed at improving their performance and extending the limits of their applicability. High electron drift velocities obtained from measurements on gas mixtures containing CF_4 (1,2) motivated us to evaluate the properties of ^3He-CF_4 and Ar-CF_4 mixtures (3) to show that these gases have the potential of improving the count rate capability, spatial resolution, and photon discrimination of neutron PSPCs (position-sensitive proportional counters) and fission counters. In support of the U.S. National Small-Angle Neutron Scattering (SANS) Facility we developed a large-area (65-cm x 65-cm) PSPC camera (4). RC position encoding (5) was chosen for simplicity of construction, but since previous experience with this encoding method had been limited to smaller PSPCs (area <25 cm x 25 cm), the main objective of this development was to show that RC encoding parameters and construction methods could be scaled up for larger area PSPCs. The use of the new counter gas mixtures enabled the development of position-sensitive transmission line fission counters (TLFCs) for neutron flux monitoring and a one-dimensional, curved PSPC for large-angle (130°) neutron diffraction experiments. The main objective of these developments was to extend the capabilities of the LC-encoding method (6,7) by mitigating the effects of interelectrode capacitance, and thereby increase the count rate capability.

*Research sponsored by the U.S. Department of Energy under contract W-7405-eng 26 with the Union Carbide Corporation.

2. NEW COUNTER GAS MIXTURES

The count rate, spatial resolution, and gamma discrimination capabilities of neutron PSPCs and fission counters are closely related to the characteristics of the counter gas and are superior for gas mixtures of higher electron drift velocity, greater stopping power for charged particles, and lower photon cross section. Furthermore, neutron counter gases should be stable under discharge conditions and in high temperature and radiation environments to prevent deterioration of the gas-kinetic properties.

Most gases of interest for the detection of thermal neutrons are mixtures of a noble gas (^{3}He, Ar, Xe) and polyatomic additives. Previously used additives (e.g. CO_2, CH_4) were selected to meet counter design requirements even though some of the abovementioned desirable properties were absent. Motivated by the work of Christophorou *et al.* (1,2), we studied the properties of CF_4 additive to ^{3}He and Ar and found CF_4 to be superior to Xe-CO_2, CO_2, or N_2 additives in gas-filled neutron counters.

We measured the electron drift velocities (w) of Ar-CF_4 and He-CF_4 as functions of the pressure-reduced electric field (E/P) and found that, compared to conventional gas mixtures (Fig. 1), the electron drift velocities of the CF_4 mixtures are considerably higher. (Although the data were obtained for ^{4}He, we expect the w values to be within 20% of those in ^{3}He.) In gases of similar stopping power and neutron cross section, the increased electron drift velocities result in shorter charge collection times and enable the use of greater signal bandwidths in the filter amplifiers to increase the count rate capability of the neutron counters. In the case of ^{3}He-filled PSPCs, the increased electron drift velocity results in better energy resolution at higher count rates and enables improved background noise reduction by pulse height discrimination. For example, we measured a 4.9% (38-keV) FWHM uncertainty in the 765-keV energy line of the ^{3}He (n_{th},p) reaction (3) using a proportional counter filled with 65% ^{3}He and 35% CF_4 at 101 kPa pressure. The avalanche charge was 0.5 pC and the pulse duration was ~2.5 μs (i.e., 640 kHz filter bandwidth). For comparison, the energy resolution of a He-Xe-CO_2 mixture of similar neutron cross section and stopping power was only 6.6% (50 keV), requiring an 8 times longer pulse duration (~20 μs).

The stopping power for protons and tritons was measured indirectly by evaluating the spatial response of a cylindrical, one-dimensional PSPC to a collimated beam of 0.1 nm neutrons (3). The spatial response to each detected neutron in this PSPC is the location of the charge centroid of the combined proton and triton trajectories from the ^{3}He (n,p) reaction. The counter gas was

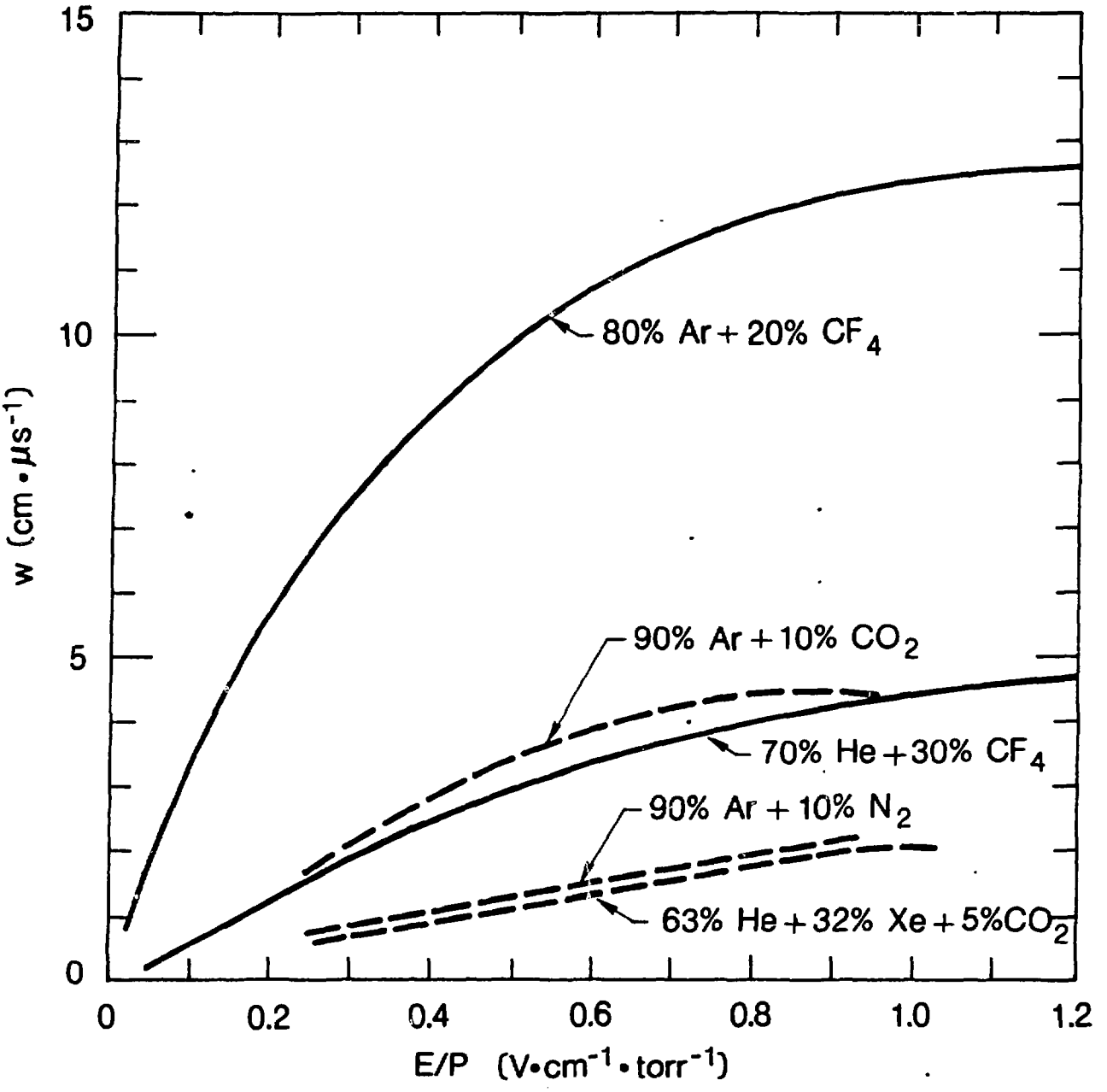

Fig. 1. The measured electron drift velocities in CF_4 gas mixtures are considerably higher than those of previously used counter gases.

65% ^3He and 35% CF_4 at 101 kPa pressure, and the counter diameter was 12.5 mm. For these conditions, the proton-triton ranges are comparable to the counter diameter; therefore, a double-peaked probability density function for the position of the charge centroids of full-energy events was measured (3). The centroid range, estimated from this probability density function, is $x_c = 3.8 \pm 0.5$ mm. This centroid range is shorter than that of 63% ^3He, 32% X and 5% CO_2 at 104 kPa, which is 5.8 ± 0.6 mm for the same neutron cross section; thus, because of the shorter centroid range, the spatial resolution of a PSPC

We tested the gamma-radiation and temperature stability of CF_4 additives by exposing a fission counter filled with 80% Ar and 20% CF_4 to a gamma radiation dose of 10^9 R at a rate of 10^6 R/h and a temperature of 523 K. We observed no degradation of the counter gas and no change in counter performance during this test; therefore, we consider the stability of this Ar-CF_4 mixture adequate for most counter environments and expect similar performance for ^{3}He-CF_4 mixtures.

The calculated photon cross section for ^{3}He-CF_4 is considerably smaller than that for ^{3}He-Xe-CO_2 of equivalent neutron cross section and stopping power (3) (e.g. at 0.1 MeV photon energy the cross section ratio for the two mixtures is ~18). The smaller photon cross section of ^{3}He-CF_4 enhances the photon discrimination and reduces the level of gamma radiation background noise.

To test the dielectric strength of the ^{3}He-CF_4 gas we increased the bias voltage (1.5•kV) until a gas multiplication factor of 10^4 (35 pC avalanche charge) was measured. Although the energy resolution had degraded considerably for this large avalanche charge, we did not observe any breakdown pulses, indicating that the dielectric strength of the He-CF_4 gas is at least comparable to the gas mixtures previously used.

3. LARGE-AREA PSPC CAMERA

A large-area (65-cm x 65-cm) camera was developed to measure the spatial coordinates of individual thermal neutrons. This camera is one of the components of the 30-m Small-Angle Neutron Scattering (SANS) Facility which has been operating since 1980 at the ORNL High-Flux Isotope Reactor. The size of the PSPC of this camera was matched to the SANS facility resolution capability; that is, a spatial resolution element (pixel) size of 1 cm x 1 cm was required to match the neutron beam diameter and scattering sample area. Other specifications for the PSPC design required a parallax error <1 pixel at a 12° scattering angle, detection efficiency >90% for 0.475 nm neutrons, a resolution matrix of 64 x 64 pixels, and a count rate capability of 10^4 s^{-1}. Furthermore, an aluminum entrance window <2 cm thick was required to mitigate neutron scattering by the PSPC.

We used the RC encoding method, selected for its simplicity and adequate spatial resolution, to meet the position sensing requirements. Basically, the PSPC is a scaled-up version of the proportional counter camera of ref. 5. The parallel anode and cathode wire planes are strung on three individual frames stacked inside the counter gas volume (4) so that the wires of the front cathode (closest to the entrance window) are parallel to the anode wires, and the wires of the rear cathode are orthogonal to the anode wires. The aluminum counter body is closed and sealed by the aluminum entrance window. Maintaining a plane

gas-window interface at 300 kPa pressure was one of the main design problems. It was solved by using a 0.8-cm-thick flat entrance window with a ^4He buffer volume at the same pressure on the opposite side. This buffer gas, which is practically transparent to the 0.475 nm neutrons, is contained by a pressure-vessel flanged disc of 1 cm thickness. The curved surface structure does not alter the PSPC characteristics because this surface is not -- as is the entrance window -- an electrode of the proportional counter. Thus, using the buffer volume, the requirements for <2 cm thickness of aluminum in the path of the neutrons and for a uniform thickness of the counter volume (i.e., uniform detection efficiency) were met.

The PSPC is filled with 63% ^3He, 32% Xe, and 5% CO_2 at 300 kPa pressure. The active thickness is 3.8 cm, resulting in a detection efficiency of 90% for 0.475 nm neutrons. The spatial resolution is ~1 cm x 1 cm FWMH at ~1 pC avalanche charge and is limited mainly by the large capacitance of ~12 pF/cm of the RC encoders. The spatial uncertainty caused by charge centroid straggling is reduced to <0.5 mm FWHM by the addition of the Xe gas at 90 kPa partial pressure. The encoder resistivity is 87 Ω/cm and the resulting spatial sensitivity is ~65 ns/cm. Using a filter amplifier bandwidth of ~53 kHz, the total signal processing time is <10 μs per detected neutron; thus the count rate capability of the PSPC is ~10^4 neutrons per second. The differential and integral nonlinearities are 12% and 2% respectively.

The background count rate not rejected by the pulse height and pulse shape discriminators (4) is <13 counts per second and is uniformly distributed over the active area of the PSPC (i.e., 0.2 counts per minute per pixel). We expect a considerable reduction of this background level (mainly gamma radiation) in an identical PSPC by substituting a 65% ^3He and 35% CF_4 mixture at 300 kPa for the presently used He-Xe-CO_2 mixture.

4. POSITION-SENSITIVE FISSION COUNTERS

The development of high temperature and high sensitivity fission counters has been an ongoing program in our group for the past six years. The motivation for the present work was to develop a fission counter with enough sensitivity [>40 counts • s^{-1} (neutrons • cm^{-2} • s^{-1})$^{-1}$ or cps/nv] to replace the BF_3 proportional counters currently used to monitor ex-vessel neutron fluxes in nuclear power plants. In this way, the source-range flux monitoring systems could benefit from such long recognized attributes of the fission counter as longer mean time between failures and the capabilities to operate at higher temperatures, in higher radiation fields, and at lower voltages than the BF_3 counterpart.

A conventional fission counter (Fig. 2) can be thought of as a parallel plate capacitor with $^{235}UO_2$-coated electrode surfaces. Neutron-induced fission reactions in the coatings cause highly ionizing fission fragments to be ejected across the gas-filled electrode gap, and subsequent electron motion in the applied electric field then induces a current pulse in the external circuit

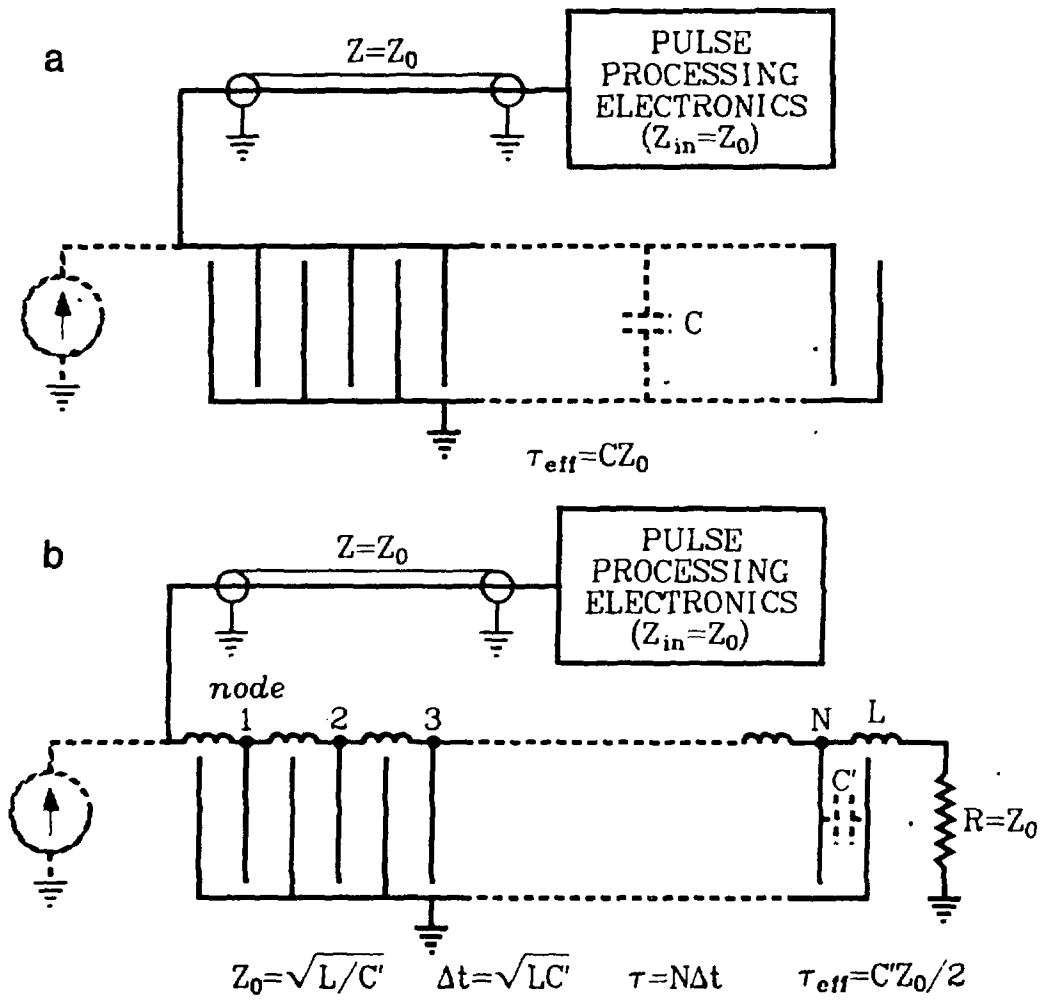

Fig. 2. Comparison of a conventional fission counter (a) and a TLFC of equal area (b). The effective capacitance of the TLFC is reduced by a factor N, and the bandwidth, $BW = (2\pi\tau_{eff})^{-1}$ is increased by a factor 2N.

(i.e., the signal cable). Alpha particles emitted from the enriched uranium coatings also ionize the gas, causing an "alpha current" even in the absence of neutron excitation. The fluctuating component of this current is random pileup noise which precludes detection of lower amplitude fission events, thereby decreasing the usable sensitivity of the counter. Fast signal processing is effective in mitigating the pileup effect but the interelectrode capacitance (C) in conjunction with the cable impedance (Z_0) constitutes a low-pass pole that

limits the signal bandwidth of the counter to $BW = (2\pi CZ_o)^{-1}$. Thus, the undetectable count rate fraction increases rapidly with electrode area due to the increasing strength of the inherent alpha source and the longer pulse durations resulting from reduced bandwidth. These considerations have limited the sensitivity of commercial fission counters to ~2.5 cps/nv.

To increase the bandwidth of large-electrode-area fission counters, we revived and expanded a method (8,9) for decreasing the effective capacitance by configuring the uranium-coated electrodes as a lumped-element LC transmission line. As can be seen in Fig. 2, the effective bandwidth of a transmission line fission counter (TLFC) is 2N times greater than that of a conventional fission counter of equal electrode area and spacing (where N is the number of nodes of the lumped-element transmission line). The recent development of low-noise, low-input impedance, wide-band preamplifiers enabled the use of low-impedance TLFCs ($Z_o \approx 25\ \Omega$) to provide bandwidths of ~100 MHz. For comparison, the bandwidths of commercial fission counters typically lie in the range of 2-10 MHz.

Induced current pulses can be generated at any one of the nodes, and, as they couple into the transmission line, approximately half of the total current propagates in each direction. However, the high electron drift velocity of the Ar-CF_4 gas mixture provides adequate pulse amplitudes in spite of this signal division. Since propagation delays are proportional to the number of nodes traversed, the position of each fission event is encoded as the difference between arrival times of the two pulses at each end of the transmission line. Each end of the TLFC is instrumented in the conventional manner with filter amplifiers and leading edge (LE) discriminators (Fig. 3). A pulse height spectrum of the time interval analyzer output (Fig. 4) shows 29 fully resolved nodes of one TLFC section. Although this position sensitivity is of minor importance for ex-vessel flux monitoring applications, it provides a means for adding another dimension of discrimination to TLFCs, which substantially reduces the lost count rate fraction. In this application, the time interval analyzer of Fig. 4 is replaced by a coincidence gate (8). The resolving time of this gate is approximately equal to the propagation delay of the TLFC. After being triggered by either discriminator, the gate generates an output only if the other discriminator also triggers within the resolving time. While fission events (which originate on a single node) satisfy this condition, most alpha pileup pulses do not. Therefore, the common threshold level of the LE discriminators can be set lower to reject fewer low-amplitude pulses.

To verify the preceding considerations, we designed a prototype TLFC with a sensitivity goal of 20 cps/nv. The sensitivity requirement of 40 cps/nv was met

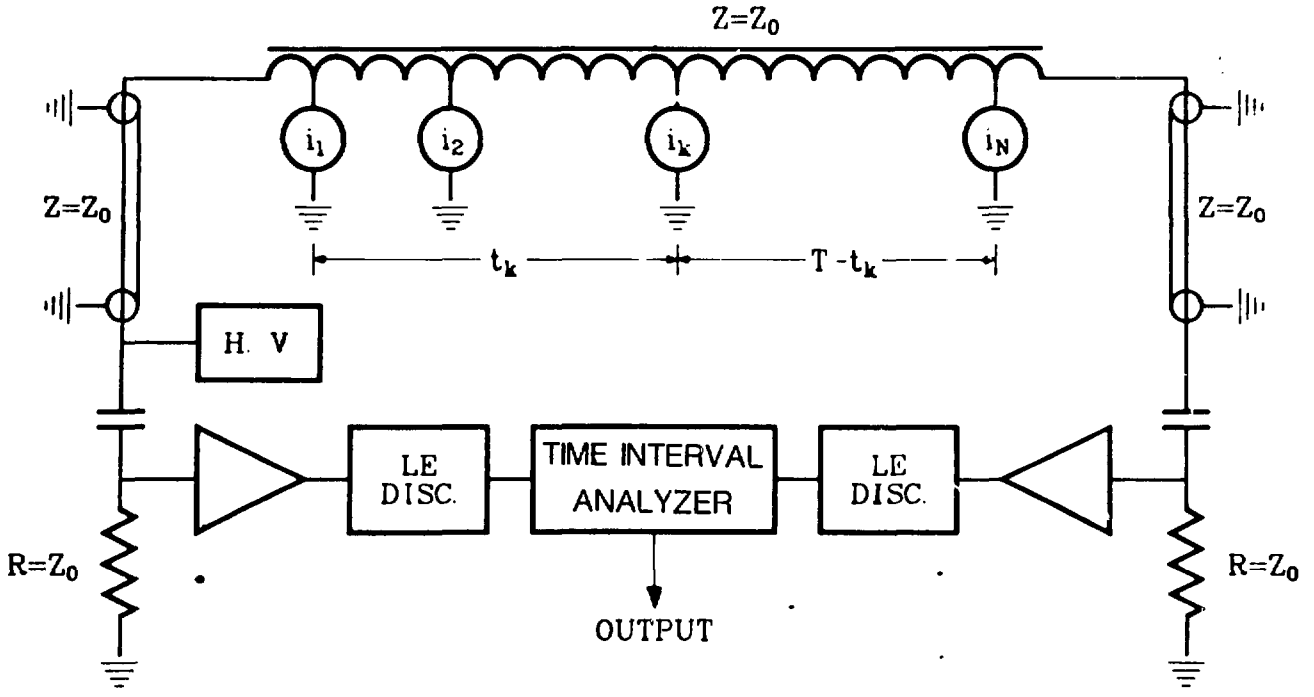

Fig. 3. The position of each fission event is encoded as the difference in arrival times of the resulting two pulses at the TLFC outputs.

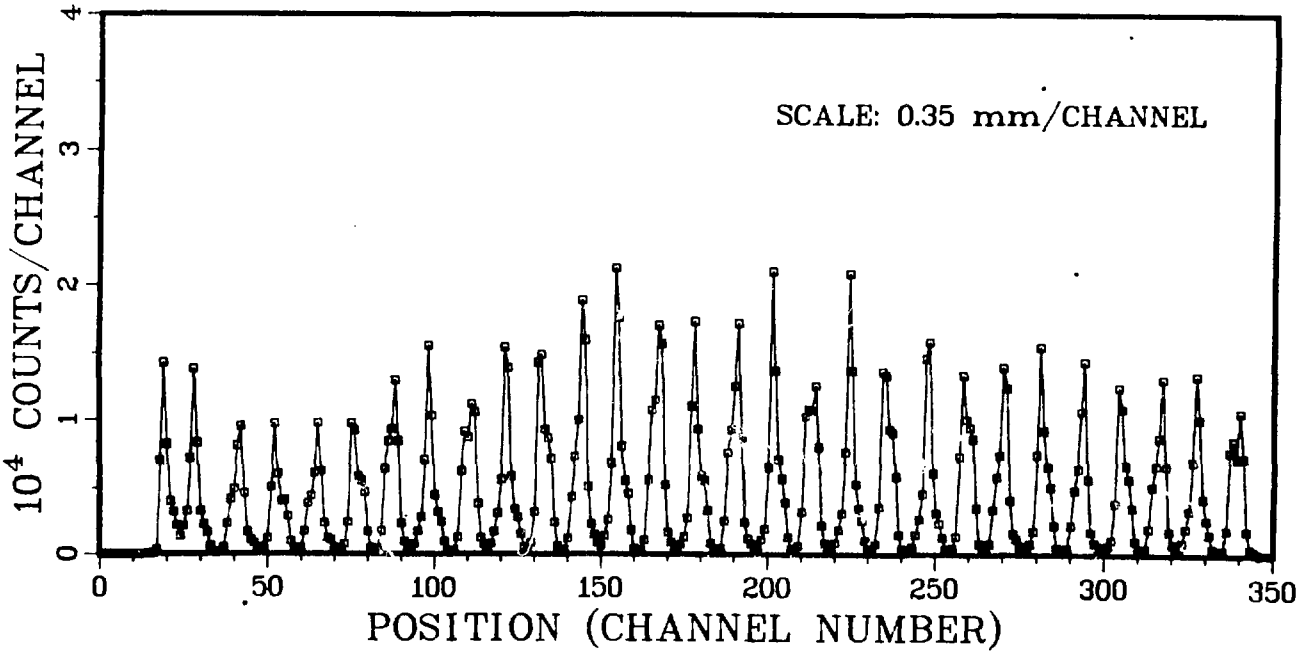

Fig. 4. The spatial resolution of a TLFC is adequate to fully resolve each node of the transmission line. The time separation between nodes is 8 ns.

by assembling two TLFCs within a common envelope. To meet size requirements (O.D. <14 cm, length <80 cm), a high electrode-packing density was realized with curved electrodes arranged about a central hub, with the electrode curvature adjusted to provide a constant electrode gap (8). Testing of this device at 453 K showed that each TLFC could provide >21 cps/nv in a 1.4×10^5 R/h gamma radiation field and >24 cps/nv at 0 R/h. Without coincidence timing, these sensitivity values must be derated by a factor of 0.6.

Another application for the TLFC which fully exploits its position sensitivity is power-range flux profile monitoring in LWRs. This function is presently accomplished with four individual fission chambers inserted to various levels in the vertical in-core instrument tubes (1.5 cm I.D.) which provide data at 1-m intervals. We have fabricated a single coaxial TLFC (4-m long by 1-cm O.D.) which will provide three times better spatial resolution over the same range. Eleven small fission counters are incorporated in the transmission line at ~0.3-m intervals, and only one end of the TLFC is cabled (Fig. 5). A short

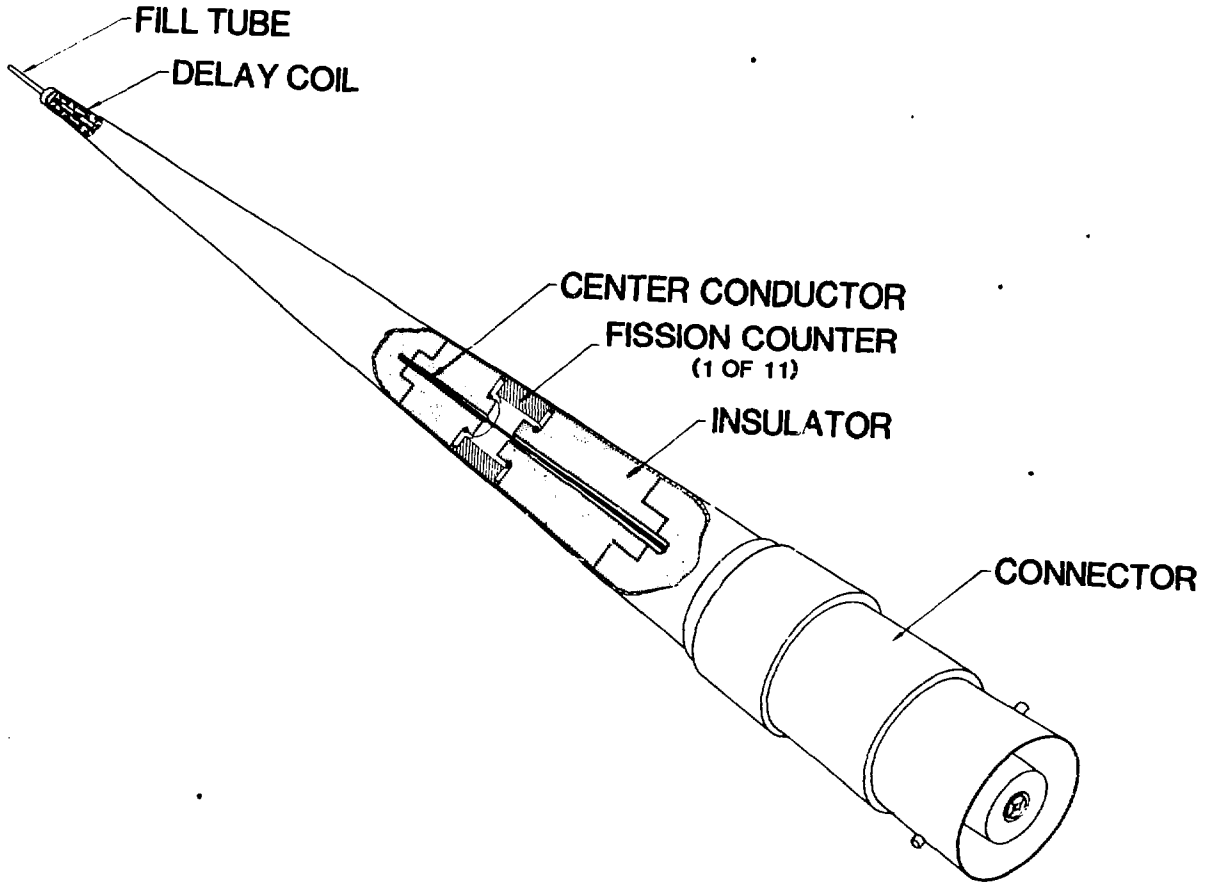

Fig. 5. Prototypic neutron flux monitor resolves 11 pixels over its 4-m length and requires only one output cable.

(~10-ns) lumped-element delay line connected to the other end is left open for pulse reflection. This additional delay permits resolution of pulse pairs originating near the open end of the delay line. After amplification, shaping, and discrimination, simple logic circuits steer the first discriminator output pulse of each pair into the start input and the second pulse into the stop input of a time interval analyzer.

5. DESIGN OF A CURVED NEUTRON PSPC

A new type of curved, one-dimensional PSPC was designed for the detection of thermal neutrons in a wide-angle neutron spectrometer to be installed at the ORNL High-Flux Isotope Reactor. The PSPC specifications require a spatial resolution of 0.2° FWHM over a 130° angle at a radius of 75 cm, a vertical sensitive height of 5 cm, a 10% count rate linearity up to 10^5 s^{-1}, and a detection efficiency of >75% for 0.13 nm neutrons. To meet these specifications, we designed a new position encoder based on a helical delay-line cathode (7).

As shown in Fig. 6, the counter electrodes are supported on a base plate and covered by a He-leak-tight enclosure. Most detected neutrons interact in the

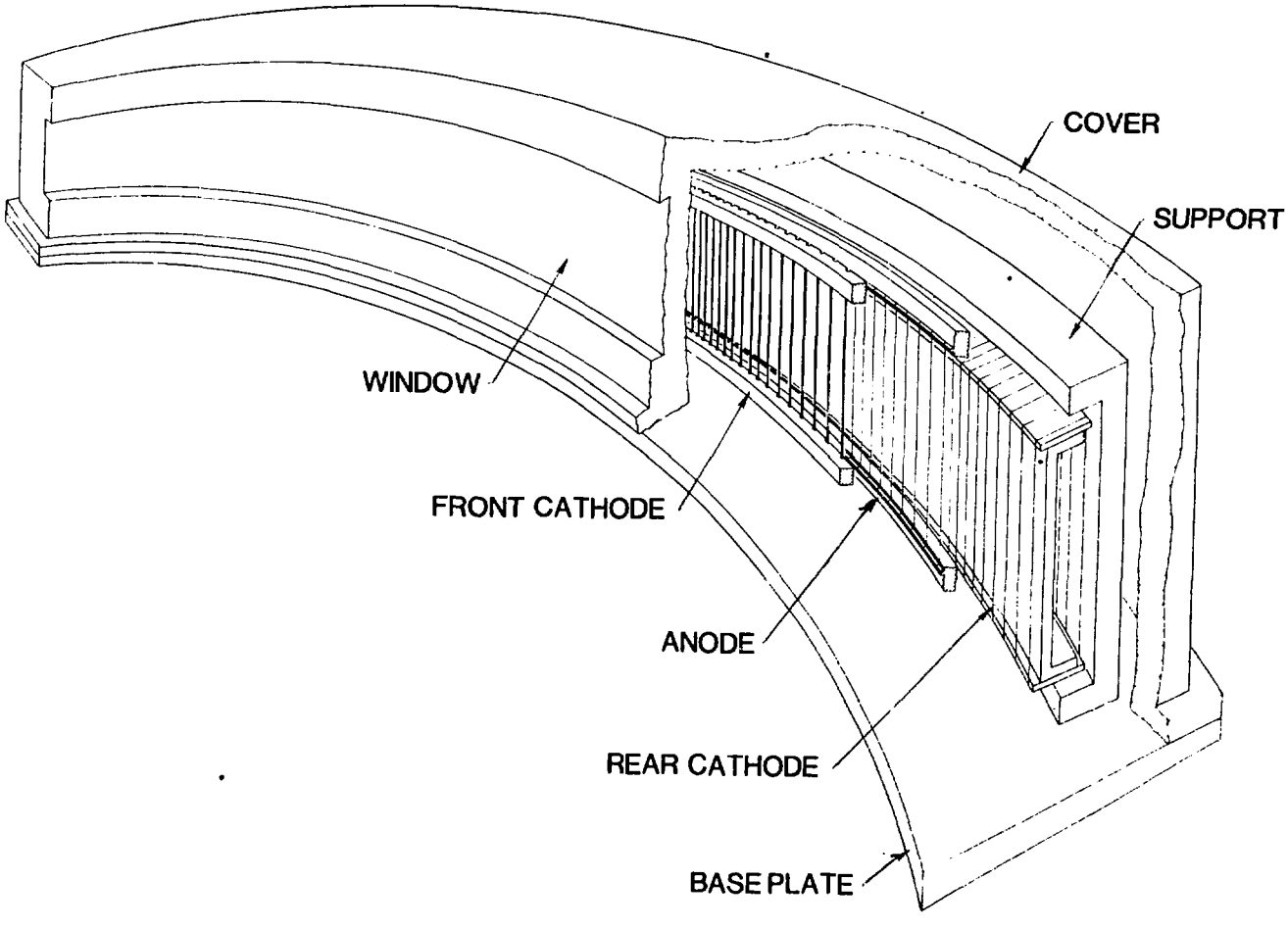

Fig. 6. Conceptual design of a curved, one-dimensional PSPC for wide-angle neutron scattering measurements uses LC position encoding.

3-cm-deep electron drift space between the 0.3-cm-thick window and the front cathode grid. Electronic ionization from the ^{3}He (n,p) interactions drifts through the front cathode toward the anode grid, where avalanche multiplication takes place. The motion of the avalanche ions away from the anode induces current pulses in the position encoder (rear cathode). As a result, two current pulses propagate through the delay line in response to each detected neutron. The time interval between the arrivals of these two signals at the output terminations is a measure of the location of the detected neutron, and the pulse height is proportional to the 765-keV Q-value of the ^{3}He (n,p) interaction.

A 41-cm-long model of the helical delay line was tested. The measured values for delay and characteristic impedance were 2.15 ns/cm and 850 Ω respectively. The bandwidth of the delay line is 3 MHz. The PSPC will be filled with 60% ^{3}He and 40% CF_4 at 600 kPa pressure for 75% detection efficiency. This mixture also provides a short (35-ns) electron collection time, which permits the use of wide-band filter amplifiers (1.6 MHz) so that the dwell time of the filtered pulses is <1 μs. Based on measurements with the model delay line, the total spatial uncertainty for an avalanche charge of 0.5 pc is expected to be <0.5 pixel (0.1° angle) FWHM.

References

1. Christophorou, L. G., Maxey, D. V., McCorkle, D. L. and Carter, J. G. (1980). *Nucl. Instrum. Methods* 171, 491.
2. Christophorou, L. G., McCorkle, D. L., Maxey, D. V. and Carter, J. G. (1979). *Nucl. Instrum. Methods* 163, 141.
3. Kopp, M. K., Valentine, K. H., Christophorou, L. G. and Carter, J. G. (1982). "New Gas Mixture Improves Performance of ^{3}He Neutron Counters", *Nucl. Instrum. Methods* , in press.
4. Abele, R. K., Allin, G. W., Clay, W. T., Fowler, C. E. and Kopp, M. K. (1981). *IEEE Trans. Nucl. Science* 28 (1), 811.
5. Borkowski, C. J. and Kopp, M. K. (1975). *Rev. Sci. Instrum.* 46, 951.
6. Valentine, K. H. (1974). "The Development of a Multiwire Proportional Chamber Imaging System for Neutron Radiography," Ph.D. Thesis, LBL-2657.
7. Lee, D. M. and Sobottka, S. E. (1973). *Nucl. Instrum. Methods* 109, 421.
8. Valentine, K. H., Kopp, M. K. and Guerrant, G. C. (1981). *Trans. Am. Nucl. Soc.* 39, 631.
9. Hess, W. N., Patterson, H. W. and Wallace, R. (1957). *Nucleonics* 15, 74.